Sensors and Materials, Vol. 34, No. 4 (2022) 1587–1599
MYU Tokyo

S & M 2912

Miniaturized Cell Fluorescence Imaging Device Equipped with Multielectrode Array

Barbara Teixeira Sais,[1†] Makito Haruta,[1*†] Kuang-Chih Tso,[1] Mizuki Hagita,[1] Takanori Hagiwara,[1] Kenji Sugie,[1] Ayaka Kimura,[2] Hironari Takehara,[1] Hiroyuki Tashiro,[1,3] Kiyotaka Sasagawa,[1] and Jun Ohta[1]

[1]Division of Materials Science, Graduate School of Science and Technology, Nara Institute of Science and Technology, 8916-5 Takayama, Ikoma, Nara 630-0192, Japan
[2]Dementia Research Unit, Osaka Psychiatric Research Center, Osaka Psychiatric Medical Center, 3-16-21 Miyanosaka, Hirakata, Osaka 573-0022, Japan
[3]Division of Medical Technology, Department of Health Sciences, Faculty of Medical Sciences, Kyushu University, 3-1-1 Maidashi, Higashi-ku, Fukuoka 812-8582, Japan

(Received November 30, 2021; accepted March 14, 2022)

Keywords: multifunctional device, lensless fluorescence imaging, electrophysiology, multielectrode array, miniaturization, cell culture

In this study, a fabrication method for a system composed of a fluorescence imaging module and a multielectrode array (MEA) chamber is described. It is important to measure both fluorescence intensity and electrical activity to obtain a better understanding of a physiological activity, such as spikes or action potentials, of cells. However, observing these physiological traits long-term with cultured cells is difficult using a conventional microscope. In this study, we developed a small fluorescence imaging device with an MEA that can be used in a conventional CO_2 incubator. The fluorescence imaging module was composed of a CMOS image sensor, a fiber-optic plate (FOP), a blue LED, and optical filters. The FOP enabled the device to be miniaturized through lensless fluorescence imaging. The MEA chamber was fabricated with micro gold electrodes deposited on the FOP. By using the FOP for the bottom of the chamber, we measured both the fluorescence signal and electrophysiology signal in the same experiment. The performance of the device was evaluated with neuronal blastoma cells. Our device enabled us to observe fluorescence images and MEA signals.

1. Introduction

Fluorescence microscopy is one of the most widely used techniques for observing the interactions of living cells.(1) Electrophysiology signals are also an important indicator of cell health and activity.(2,3) However, there is no precise, reliable method for determining the relationship between fluorescence intensity and electrophysiological cell depolarization voltage. A reliable method that can quantify fluorescence signals is highly desirable. Although multiple techniques allow us to measure both signals separately, the reliability of the data is reduced by

*Corresponding author: e-mail: m-haruta@ms.naist.jp
†These authors contributed equally to this work.
https://doi.org/10.18494/SAM3758

ISSN 0914-4935
https://myukk.org/

the slight difference in position of the two measurements, even if made on the same sample, preventing the comparison between the fluorescence signal and electrophysiological signal from the same cell. Also, moving the sample will change the environmental conditions of the sample or cell culture. Another disadvantage of separate measurements is that they are normally performed outside the incubator owing to the size of the equipment, which means that the cells are not in their perfect physiological condition.[4] We previously developed a portable imaging system for cell culture experiments[5] and a highly sensitive lens-free imaging device using a CMOS image sensor.[6]

In this study, we present a small device capable of recording both signals simultaneously. We used a multielectrode array (MEA) to record the *in vitro* electrical activity of neuronal cells under physiological conditions. The microelectrodes were fabricated on a fiber-optic plate (FOP) substrate using conventional microfabrication processes, such as photolithography, metal and insulator deposition, and etching. In the following sections, the design and fabrication process for both the MEA and the imaging module are described, as well as our initial results.

2. Materials and Methods

2.1 Miniaturized cell fluorescence imaging device

We developed a miniaturized cell fluorescence imaging device equipped with an MEA for observing fluorescence signals and electrophysiological signals [Fig. 1(a)]. This device can be used in a conventional CO_2 incubator for long-term observations of cultured cells. This device has two main structures: a fluorescence imaging module with a CMOS image sensor, and a special cell culture chamber that is assembled on the surface of the MEA.

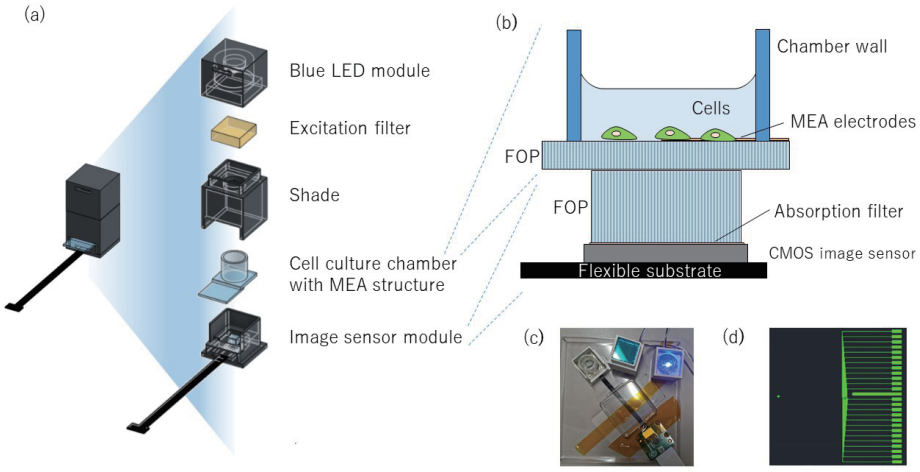

Fig. 1. (Color online) Overview of instrumentation in study. (a) Fabricated device composed of LED module, excitation filter, shading structure to protect the device from external light, cell culture chamber on the MEA structure, and image sensor module; (b) diagram of the assembled cell culture chamber with MEA structure and image sensor module; (c) photograph of the assembled imaging system; and (d) designed mask pattern.

2.2 Imaging module

The imaging module was composed of a CMOS image sensor (Sony IMX219, B07HMZ9ZFX, Sain Smart, US) with 3280 × 2464 pixels, a FOP (J5734, Hamamatsu Photonics, Japan), a blue LED (OSB5XAAC11U, OPTOSUPPLY, China) with an emission wavelength of 465–475 nm, and optical filters (Ex 450 nm, Em 500 nm) as shown in Figs. 1(a) and 1(b). The FOP enabled the miniaturization of the device through lensless fluorescence imaging. The FOP was composed of a bundle of micron-sized optical fibers, each with a diameter of 3 μm. The FOP was pasted on the surface of the absorption filter (500-nm-long pass) and directly mounted on the face of the CMOS image sensor. A Raspberry Pi (4B, Raspberry Pi Foundation, UK) and a Python program (Python Software Foundation, US) controlled the CMOS image sensor (Fig. 2). The excitation light source was composed of an excitation filter (CLW 450 ± 2 nm, FB450-10, Thorlabs, Inc.) and an LED. A thin layer of fiber-connecting gel was applied between the image sensor and the FOP substrate to decrease the gap between them.

2.3 Cell culture chamber with MEA

We used 25 electrodes in a square distribution on a square FOP substrate of 1.5 cm side length and 1 mm thickness. The diameter of the electrodes was 30 μm and the distance between them was 60 μm. Twenty-six rectangular contact pads (25 for each electrode and one for reference) were designed with dimensions of 1 × 0.3 mm^2, with the exception of the reference electrode, which had a semicircular tip with a radius of 15 μm attached to a rectangle of 5 × 0.3 mm^2.

Several points were considered when choosing the fabrication materials, such as biocompatibility, signal disturbance, and the imaging module to be placed underneath the electrical measurement module. Because our goal was to develop a system capable of recording both cell images and cell signals, a FOP was used as our substrate. Because the optical fibers convey the incident image to the output surface, the FOP was ideal for our requirements.[7] Gold was used for the electrodes because of its biocompatibility, resistance to corrosion, longevity,

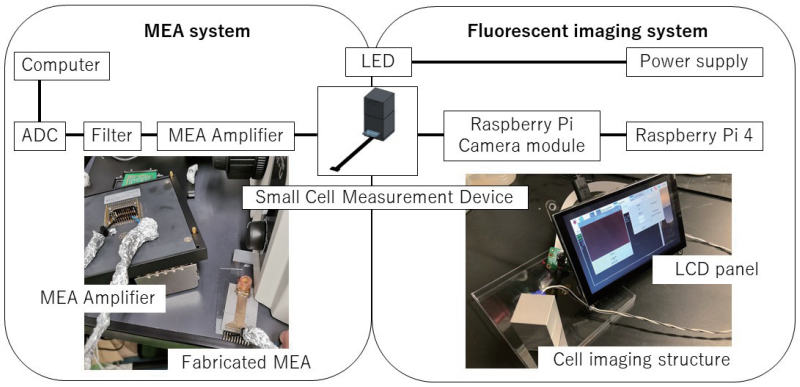

Fig. 2. (Color online) Setup used to acquire electrophysiological signals.

and high conductivity.[8,9] To enhance the adhesion of the gold electrodes on the substrate, a buffer layer of aluminum was used. To prevent voltage leakage and interference between the channels, an electrical insulator should be used.[9,10] Parylene C has an inert surface and a low dielectric constant (2.95),[11] and was thus used in this study as an insulator.[12,13]

To fabricate the MEA, the FOP substrate was first cleaned in an oxygen plasma machine. A standard photolithography process was then performed using LOR2B and OFPR 8600 as positive photoresists with designed MEA patterns. The layout of the designed MEA pattern is shown in Fig. 1(d). Sequentially, a 30 nm layer of aluminum was deposited, followed by a 300 nm gold layer. A lift-off process was then performed at 60 °C for 30 min, using acetone and Remover PG to remove the OFPR 8600 and LOR2B layers. After that, a silane coupling treatment was performed to improve the adhesion between the gold MEA and the subsequently deposited Parylene C insulator layer with a thickness of around 2 μm. Because the insulator was uniformly deposited over the entire substrate surface, including the electrodes and pads, another photolithography process was performed using a mask designed to open these structures. For this process, THMR photoresist was used because it provides a thicker film and requires a lower baking temperature than OFPR 8600. Finally, plasma treatment with oxygen gas and etching with acetone were performed. Figure 3 illustrates the step-by-step process. After the final etching process, a 1-cm-diameter acrylic tube cut to a length of 1 cm was placed on the MEA with the electrodes at the center of the tube. The well formed by the tube adhered on the substrate was used as the cell culture chamber as shown in Figs. 1(a) and 1(b). Figure 1(c) shows a photograph of the fabricated device.

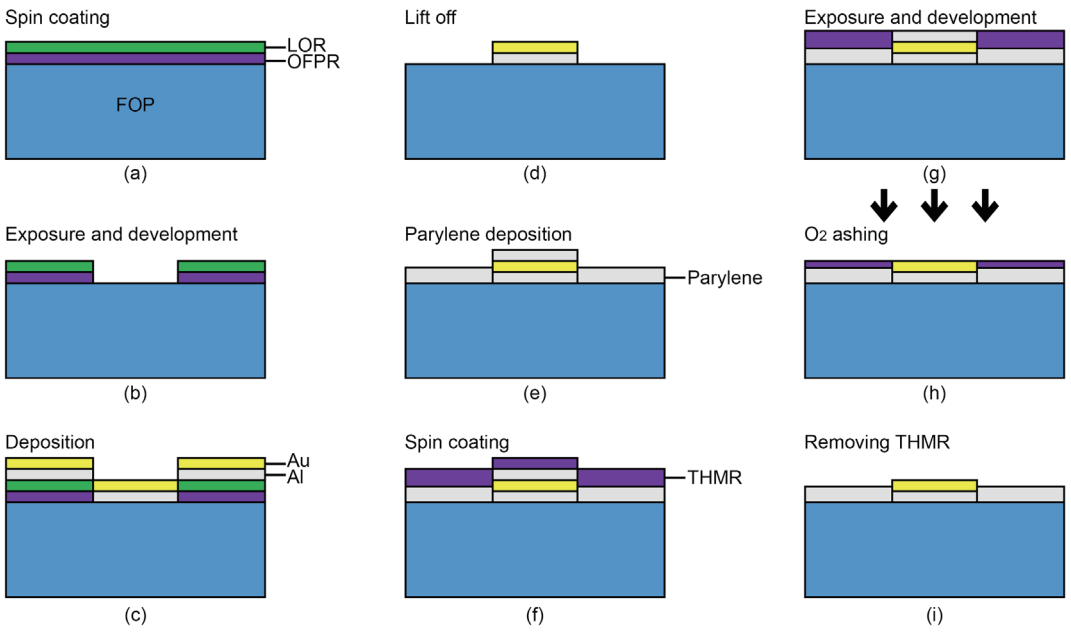

Fig. 3. (Color online) Process used for MEA fabrication. (a) Spin-coating of LO2RB and OFPR 8600 photoresists, (b) mask patterning (electrodes and wires), (c) Al/Au deposition, (d) lift-off process, (e) Parylene C coating, (f) THMR deposition, (g) mask patterning (opening electrodes), (h) final structure with THMR, and (i) THMR removal.

The sample was then left to dry for 24 h at room temperature. Then, the pads of the sample were bonded to the flexible substrate. The wires were also covered in epoxy resin for protection. After the connection to the flexible substrate had been secured by epoxy resin, a header pin was attached to the end of the substrate.

2.4 Cell culture

To enhance biocompatibility, the cell culture chamber was washed with Terg-a-zyme® detergent (Z273287; Sigma-Aldrich) and left overnight inside an incubator at 37 °C. After that, a 10 mM trypsin (R001100; ThermoFisher) solution was prepared and added dropwise to the cell chamber well. The MEA was then placed in a fridge (4 °C) for 2 h.

NG108-15 cells (Cell Bank, Tohoku University) were seeded at an initial density of 2×10^6 cells/mL and nourished in a cell medium composed of DMEM+GlutMax (10566-016; ThermoFisher) + 10% FBS (SH30071.03; ThermoFisher). The medium was exchanged completely every 24 h. The cells were cultured for 3 days before the MEA signal was measured.

2.5 Fluorescence imaging and image processing

To acquire fluorescence images, the cells were stained with Fluo-8 AM dye (1345980-40-6; AAT Bioquest) for 45 min prior to image acquisition. The obtained fluorescence image had low differentiation in its raw state and, thus, imaging processing was performed on it. Firstly, a general histogram stretch was carried out to improve contrast in the image. After that, a 7 × 7 region of interest (ROI) was defined to look for points of intensity that distinguished themselves (+2 is the signal variance) from the ROI's histogram average. If pixels with these qualities were found, they were marked and the histogram was stretched to increase the difference between them and the background. The pixels surrounding the classified indexes that exhibited at least 30% of their intensity were classified as also belonging to the fluorescence group, and the histogram was stretched accordingly. This step was made to ensure that pixels affected by the light scattering were not incorrectly classified.

2.6 MEA recoding and signal processing

To measure the signal from our fabricated multielectrode array, we connected the pins of our output connector to the input connector of a commercial MEA system (MEA1060-Inv-BC, Multichannel Systems). This system was connected to a filter (FA64, Multichannel Systems) and then to the spike detection system. The software Spike2 was used to measure the spontaneous spike activity. Figure 2 shows the setup.

The signal was obtained at a 10 kHz sampling rate and a 10k gain for 5 h. A high-pass digital filter (cutoff frequency 200 Hz) was applied to the signal during recording.

The signal was measured in three instances: (i) the MEA with no cell activity and only PBS in the cell chamber; (ii) the MEA with a cell culture in its cell chamber; and (iii) cells stimulated with 100 µl of 1 M KCl. The first measurement was made to define the baseline signal and the

noise inherent to our system. Stochastic signal processing[14] was performed on the acquired signal; then, a Z-score algorithm[15] was used to extract the neuronal spike signals from the measured cell signal.

Stochastic signal processing is used to describe and manipulate random signals, and therefore processes. A random process is composed of, on one side, an infinite number of random variables, indexed by a time index n, which are triggered in turn and produce, on the other side, a set of samples that can be measured, regardless of the transfer function. Because the variables are random, the generated signal will be different every time. However, by definition, these variables are still sufficiently similar that they can be considered to belong to the same group, such as spike signals. When such variables are added to another signal that is sufficiently random to not be easily deconvoluted but sufficiently predicable for some pattern to be found, a method of separating these signals is to analyze the statistical relation between the values. To analyze the recorded signal, which was highly noisy due to the instrumental configuration, a *k*th-order description approach was used with a second-order description, which means that the time-varying mean and time-varying autocorrelation were analyzed in a predefined window of 3 s. A quadratic cost function was applied to the signal. To define the baseline of the function, we measured the signal of our MEA with no cells in the chamber and only with PBS for approximately 5 h. The signal with the cells was then measured, and the probability curves and costs were compared to define the windows where spikes occurred. Because this method relies on probability to infer the behavior of a signal, and our signal was composed of a weak part of interest (spikes) and a strong random signal (instrumental noise), this processing might have caused spike signals to be overlapped with noise on multiple occasions, affecting the accuracy of our measurement system, a point that will be returned to in the discussion.

3. Results

3.1 MEA structure

After the epoxy had dried and the connection wires were secured, we analyzed the fabricated structure by microscopy and using our imaging device. Figure 4 shows a diagram of the final structure of the fabricated MEA [Fig. 4(a)], a photograph of the fabricated sample [Fig. 4(b)], a micrograph of the MEA electrodes obtained with 10× magnification [Fig. 4(c)], and a bright-field image captured by our imaging system [Fig. 4(d)].

3.2 MEA signal measurement

After preparing the cell chamber with trypsin and culturing the cells for 72 h, the electric signal of our system was measured. For this purpose, a double-ended IC clip cable, covered in aluminum foil to decrease noise, was used. The pins from our header pin were connected to the output pins of the commercial MEA system, as shown in Fig. 3. Figure 5 shows a bright-field image of the cell culture used for signal measurement obtained with our device [Fig. 5(a)] and the results after signal processing and spike recognition under normal [Fig. 5(b)] and stimulation

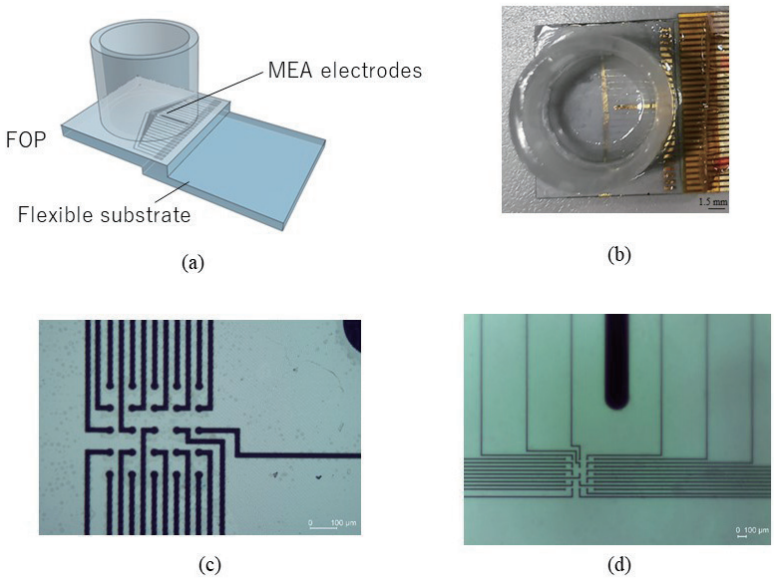

Fig. 4. (Color online) Final structure of the fabricated MEA. (a) Schematic of the cell signaling structure. (b) Photograph of the fabricated device taken with a smartphone. (c) Micrograph of the fabricated MEA electrodes with 10× magnification. (d) Bright-field image captured by our device.

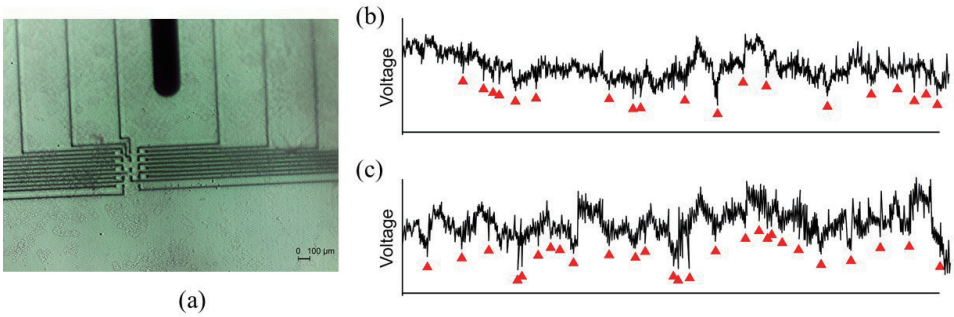

Fig. 5. (Color online) Signal after stochastic processing and spikes detected with the Z-score algorithm. (a) Cell culture on the FOP. (b) Electrophysiological signal recorded without stimulus. The red triangles indicate the spikes recognized by the algorithm. (c) Signal and spikes recorded when stimulating the cells with KCl.

[Fig. 5(c)] conditions. The recorded signal intensity was 122.8 ± 38.3 μV. When stimulated, the cells showed an increase in intensity of 8.5 ± 4.2 μV and an increase in the firing rate of 13%.

3.3 Fluorescence images

After assembling the image sensor and adding a thin layer of optical gel to it, bright-field and fluorescence images were obtained. For this purpose, cells were cultured for 3 days in a CO_2 incubator. One hour before the experiment, the cell culture medium was removed and replaced

with PBS to avoid background noise when acquiring the fluorescence signal. A fluorescent dye was then added to it, and the mixture was incubated for 45 min at 37 °C. Figure 6 shows the resulting images obtained with our system and a microscope as both bright-field and fluorescence micrographs. Firstly, micrographs with 4× magnification were taken of both bright-field [Fig. 6(a)] and fluorescence images [Fig. 6(b)] and used as gold standards to ensure the accuracy of our device. With our device, a bright-field image [Fig. 6(c)] was recorded to secure the cell position during fluorescence signal imaging. For the fluorescence image [Fig. 6(d)], parameters such as exposure time and excitation light intensity were adjusted while checking the obtained data. Lastly, the fluorescence images were processed to enhance them [Fig. 6(e)].

To verify the device response when cells were stimulated, 100 µl of KCl at a concentration of 1 M was added to the cell chamber. KCl can promote neuronal stimulation as it causes depolarization and activation of voltage-gated receptors. As shown in Fig. 7, firstly, the bright-field image [Fig. 7(a)] was recorded, followed by the fluorescence signal without the addition of

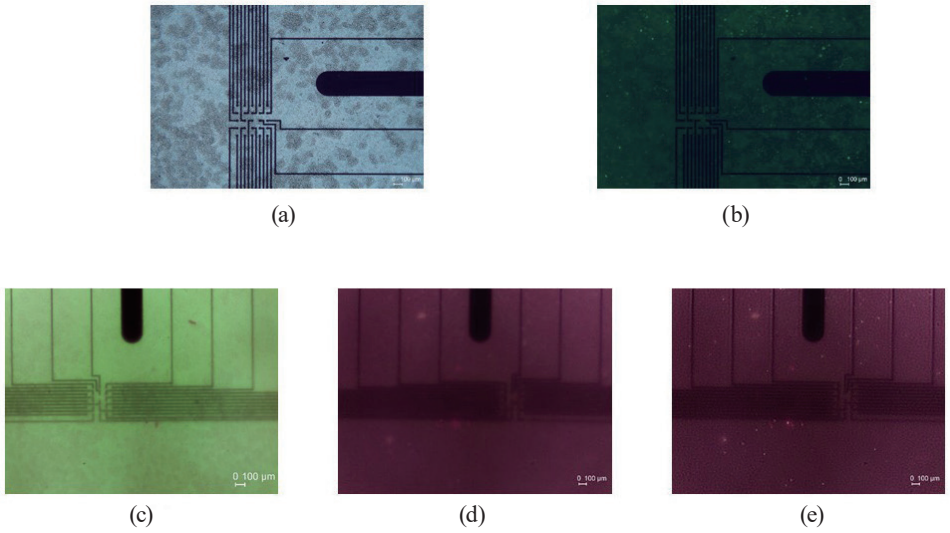

Fig. 6. (Color online) Images obtained with our imaging system. (a) Bright-field micrograph obtained with 4× magnification. (b) Fluorescence micrograph obtained with 4× magnification. (c) Raw bright-field image obtained with our device. (d) Raw fluorescence image obtained with our device. (e) Processed fluorescence image obtained with our device. A local-window deviation method was applied to the raw images to identify the brighter pixels.

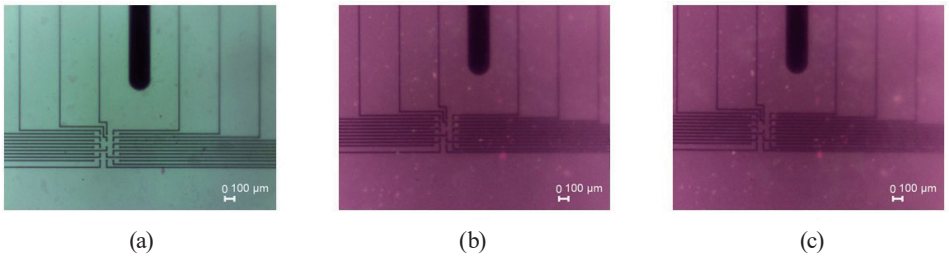

Fig. 7. (Color online) Captured images after cell stimulation with KCl. (a) Bright-field image of the cell chamber. (b) Fluorescence image before KCl stimulation. (c) Fluorescence image after KCl stimulation.

KCl [Fig. 7(b)] and, finally, the fluorescence signal while stimulating the cells with KCl [Fig. 7(c)]. The signal captured after stimulation had an intensity 16 ± 3.5% higher than that of the physiological signal.

4. Discussion

In this work, a small device composed of both electrophysiological and fluorescence signal recording modules was fabricated. To fabricate the electrophysiological module, a standard positive photolithography method was used. Because we wanted to record signals from living cells, biocompatibility and cell toxicity were factors to be considered. Also, conductivity, electrical properties, and durability were characteristics of interest. Owing to its stability and longevity, gold was chosen to fabricate the electrodes. Despite its low impedance, gold is a good alternative to platinum as it is suitable for coating medical instruments and has high conductivity and cell compatibility. It was ensured that all other used materials were biocompatible, optically transparent, and inert so as not to interfere with the physiochemical cell culture environment. The electrode and interconnection size were also parameters of interest. The interconnection size was especially relevant during the lift-off process as a very narrow path made this process difficult. Because the aim of this study was to fabricate a device capable of correlating cell electrical signals and fluorescence intensity, a FOP was chosen as the substrate for our MEA. The FOP has the properties of inertness and optical transparency, with the advantage of allowing an image formed on its upper face, on which the MEA was fabricated, to be transmitted without distortion to the output face, directly under which an image sensor was located. This allowed us to capture both bright-field and fluorescence images satisfactorily. For the imaging module, several other focuses of attention were the excitation light brightness, excitation filter cutoff wavelength, and sensor resolution. A lack of power of the excitation light will result in a low or inexistent fluorescence signal, whereas a very strong power will result in a poor-quality image due to low pixel differentiation. The filter wavelength directly influences the fluorescence intensity, signal quality, and fluorescence dye selection. Finally, the image sensor resolution is relevant for signal recording and structure identification.

4.1 MEA structure and signal

The fabricated MEA was robust, being able to undergo washing and sterilization in an autoclave (120 °C, 30 min) and remain for long periods of time inside the incubator (37 °C, approximately 72 h) without any fracture on the electrodes. The acrylic tube used as the walls of the cell chamber also did not show any detachment from the substrate surface. The device showed good biocompatibility, with 88% of the cells showing viability at the end of the third incubation day. This percentage provided us with a sufficiently strong signal to be measured by our system, although the biocompatibility issue should be studied further. Regarding the measured signal, the noise found in the measurement was high and required heavy digital data processing, such as a stochastic method, which inherently destroyed part of the measured electrophysiological signal and made spike identification difficult. The majority of the noise

originated from the setup used to connect our device's output to the input of the commercial MEA system. Because of the limitations of the connection method, we analyzed the average signal, obtained from the sum of the recordings of all 25 electrodes, as it was not possible to analyze the signals from individual electrodes.

The next steps in this work are to construct a measurement system coupled to our MEA to reduce the noise in the system and achieve single-electrode signal recording, and to fabricate a stimulation module.

4.2 Cell imaging system

For the image module, both bright-field and fluorescence images were successfully obtained. Parameters such as excitation light intensity and exposure time were refined and selected so as to maximize the signal recorded. For fluorescence images, an image processing algorithm was performed to enhance pixel differentiation, but fluorescence signals were satisfactorily obtained. The imaging system was able to satisfactorily capture fluorescence data from NG108-15 cells stained with Fluo-8 AM dye. Even without processing, the images showed promising results.

5. Conclusions

In this study, we designed and fabricated a compact MEA on a FOP substrate with 25 electrodes of 30 μm diameter. The fabrication process employed the standard positive lithography process, using OFPR 8600 and THMR as photoresistors, aluminum and gold films as the electrodes, and a Parylene C coating as an insulator. The FOP substrate was used because of its image transmission property, as we also aimed to obtain fluorescence images from the cells taken. The surface of the cell chamber was treated with trypsin to increase its biocompatibility. To measure the electrophysiological signal from the cells, we connected our device to a commercial MEA system. Even with the high noise level obtained by this configuration, we were still able to record and identify spontaneous spikes. The imaging module also proved to be highly satisfactory. The system was designed to be sufficiently compact to fit inside an incubator. With this setup, the simultaneous acquisition of spike activity and fluorescence signals is possible. Simultaneous signal acquisition can help investigate neuronal dynamics and possibly establish the relationship between fluorescence and action potentials. Future works involve (i) the fabrication of a measurement signal module to be coupled directly to our system to decrease the noise level; (ii) signal measurement from single electrodes; (iii) the fabrication of a stimulation module; and (iv) the simultaneous acquisition of electrophysiological signals and fluorescence images inside the incubator.

Acknowledgments

This study was supported by the Japan Society for the Promotion of Science (JSPS) (19K16883, 18H03780).

References

1 A. Caricati-Neto and L. B. Bergantin: Nucl. Med. Biomed. Imaging **2** (2017) 1. https://doi.org/10.15761/NMBI.1000124
2 M. E. Spira and A. Hai: Nat. Nanotechnol. **8** (2013) 83. https://doi.org/10.1038/nnano.2012.265
3 P. Massobrio, J. Tessadori, M. Chiappalone, and M. Ghirardi: Neural Plast. **2015** (2015) 196195. https://doi.org/10.1155/2015/196195
4 R. B. Clark, T. A. Schmidt, F. B. Sachse, D. Boyle, G. S. Firestein, and W. R. Giles: J. Physiol. **595** (2016) 635. https://doi.org/10.1113/JP270209
5 A. Wuthayavanich, M. Haruta, H. Takehara, T. Noda, K. Sasagawa, T. Tokuda, and J. Ohta: Sens. Mater. **28** (2016) 1317. https://doi.org/10.18494/sam.2016.1401
6 K. Sasagawa, A. Kimura, M. Haruta, T. Noda, T. Tokuda, and J. Ohta: Biomed. Opt. Express **9** (2018) 4329. https://doi.org/10.1364/BOE.9.004329
7 M. Haruta, Y. Kurauchi, M. Ohsawa, C. Inami, R. Tanaka, K. Sugie, A. Kimura, Y. Ohta, T. Noda, K. Sasagawa, T. Tokuda, H. Katsuki, and J. Ohta: Biomed. Opt. Express **4** (2010) 1557. https://doi.org/10.1364/BOE.10.001557
8 R. Kim, N. Hong, and Y. Nam: Biotechnol. J. **8** (2013) 206. https://doi.org/10.1002/biot.201200219
9 E. Seker, Y. Berdichesvsky, M. R. Begley, M. L. Reed, K. J. Staley, and M. L. Yarmush: Nanotechnology **21** (2010) 125504. https://doi.org/10.1088/0957-4484/21/12/125504
10 M. E. J. Obien, K. Deligkaris, T. Bullman, D. J. Bakkum, and U. Frey: Front. Neurosci. **9** (2015) 8. https://doi.org/10.3389/fnins.2014.00423
11 Diamond-MT Conformal Coating: https://blog.paryleneconformalcoating.com/parylene-dieletric-properties/ (accessed September 2021).
12 H. Kang, Y. Nam: Stretchable bioelectronics for medical devices and systems (Springer, Cham, Switzerland, 2016) 1st ed., pp. 69–82.
13 PCI Paint & Coating Industry: https://www.pcimag.com/articles/87074-parylene-coatings-and-applications. (accessed September 2021).
14 A. Papoulis and S. Unnikriahna Pillai: Probability, Random variables, and stochastic process (McGraw-Hill, New York, 2002) 4th ed., pp. 243–629.
15 Y. Cao, S. K. Maran, M. Dhamala, D. Jaeger, and D. H. Heck: J Neurosci. **32** (2012) 8678. https://doi.org/10.1523/JNEUROSCI.4969-11.2012

About the Authors

Barbara Teixeira Sais received her B.S. and M.S. degrees from the Federal University of Sao Paulo (Biomedical Engineering, 2017 and Graduate Program of Biomedical Engineering, 2019). She is currently pursuing her Ph.D. degree at Nara Institute of Science and Technology (NAIST). Her major research interests are biological and medical signal recording and processing. (teixeira.sais_barbara.tq2@ms.naist.jp)

Makito Haruta received his B.E. degree in bioscience and biotechnology from Okayama University, Okayama, Japan, in 2009 and his M.S. degree in biological science and Dr. Eng. degree in material science from Nara Institute of Science and Technology (NAIST), Nara, Japan, in 2011 and 2014, respectively. He was a postdoctoral fellow with NAIST from 2014 to 2016. He joined the Institute for Research Initiatives, NAIST, in 2016, as an assistant professor. In 2019, he joined the Graduate School of Science and Technology, NAIST, as an assistant professor. His research interests include brain imaging devices for understanding brain functions related to animal behaviors.

Kuang-Chih Tso received his B.S. and M.S. degrees from National Chiao Tung University (Applied Chemistry, 2015 and Graduate Degree Program of Science and Technology of Accelerator Light Sources, 2017). He worked at Lam Research Inc. as a processing engineer on a project of advanced interconnect fabrication. He is currently pursuing his dual Ph.D. degree in materials science and engineering from Nara Institute of Science and Technology and National Yang Ming Chiao Tung University. His major research interests are bio-electrode fabrication, implantable retinal devices, and microstructural analysis in National Synchrotron Radiation Research Center.

Mizuki Hagita received her B.S. degree in science and technology from Akita University, Japan, in 2020. Currently, she is in the final year of her master's degree at Nara Institute of Science and Technology, Japan. Her research interests include the development of flexible devices for retinal prosthesis.

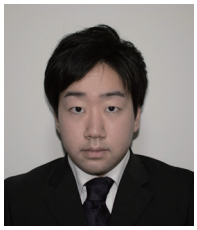

Takanori Hagiwara received his B.E. degree from the National Institute of Technology, Maizuru College, Japan, in 2021. Currently, he is in the first year of his master's course at Nara Institute of Science and Technology, Japan. His research interests are in retinal prosthesis devices.

Kenji Sugie received his B.S. degree in electrical and electronic engineering from Ritsumeikan University, Shiga, Japan, and his M.E. degree from Nara Institute of Science and Technology (NAIST), Nara, Japan. He is currently pursuing his Ph.D. degree at NAIST at the Photonic Device Science Laboratory. His research interests include implantable devices for neural activity observation.

Ayaka Kimura received her B.S. degree in applied biological sciences from Tokyo University of Agriculture, Japan, in 2010, her M.S. degree in biological sciences from Nara Institute of Science and Technology, Japan, in 2012, and her Ph.D. degree in medical science from Kyushu University, Japan, in 2018. In 2017, she joined Nara Institute of Science and Technology as a researcher. She was a postdoctoral fellow at Jikei University School of Medicine from 2019 to 2020. She has been a project team leader at Osaka Psychiatric Medical Center since 2020. Her research interests are in behavioral neuroscience and dementia.

Hironari Takehara received his B.E. and M.E. degrees in applied chemistry from Kansai University, Osaka, Japan, in 1984 and 1986, respectively, and his Ph.D. degree in materials science from Nara Institute of Science and Technology (NAIST), Nara, Japan in 2015. From 1986 to 2012, he was a semiconductor process engineer at Panasonic Corporation, Kyoto, Japan, where he developed BiCMOS, high-voltage SOI, and optoelectronic IC processes. In 2015, he joined NAIST as a postdoctoral fellow and became an assistant professor in 2019. His current research interests involve CMOS image sensors and bioimaging. (t-hironari@ms.naist.jp)

Hiroyuki Tashiro received his B.E. and M.E. degrees in electrical and electronic engineering from Toyohashi University of Technology (TUT), Aichi, Japan, in 1994 and 1996, respectively. He received his Ph.D. degree in engineering from Nara Institute of Science and Technology (NAIST), Nara, Japan, in 2017. In 1998, he joined Nidek Co., Ltd., Aichi, Japan, where he worked on the research and development of ophthalmic surgical systems and retinal prostheses. In 2004, he joined the Faculty of Medical Sciences, Kyushu University, Fukuoka, Japan, as an assistant professor, and since 2019 has also been an associate professor at NAIST. His current research interests include artificial vision systems and neural interfaces.

Kiyotaka Sasagawa received his B.S. degree from Kyoto University, Kyoto, Japan, in 1999, and his M.E. and Ph.D. degrees in materials science from Nara Institute of Science and Technology (NAIST), Nara, Japan, in 2001 and 2004, respectively. From 2004 to 2008, he was a researcher with the National Institute of Information and Communications Technology, Tokyo, Japan. In 2008, he joined NAIST as an assistant professor, where he has been an associate professor since 2019. His research interests include bioimaging, biosensing, and electromagnetic field imaging.

Jun Ohta received his B.E., M.E., and Dr. Eng. degrees in applied physics from The University of Tokyo, Japan, in 1981, 1983, and 1992, respectively. In 1983, he joined Mitsubishi Electric Corporation, Hyogo, Japan. From 1992 to 1993, he was a visiting scientist with the Optoelectronics Computing Systems Center, University of Colorado Boulder. In 1998, he joined the Graduate School of Materials Science, Nara Institute of Science and Technology (NAIST), Nara, Japan as an associate professor. He was appointed as a professor in 2004. His current research interests include smart CMOS image sensors for biomedical applications and retinal prosthetic devices. He is a fellow of IEEE, the Japan Society of Applied Physics, and the Institute of Image, Information, and Television Engineers. He serves as an associate editor of IEEE Transactions on Biomedical Circuits and Systems and on the editorial board of Journal of Engineering, IET.